PROCEEDINGS OF SCIENCE

Status of defect investigations

A. Junkes[*][†]
University of Hamburg
E-mail: alexandra@junkes.dk

The origin of sensor deterioration in silicon tracking detectors in high energy physics experiments is to a large proportion a result of crystal defects in the silicon bulk. These defects can be analysed and identified with the aim to eventually find the best possible material or even a "cure" for the impact of these defects. In the recent years, these studies have been performed on n-type silicon sensors that were irradiated with neutrons, pions, protons, electrons and ^{60}Co-γ. This work's main focus is set on neutrons and charged hadrons, since these particles are the dominant source of radiation damage in future large hadron collider (LHC) experiments.
To date, two defects were found to be responsible for the generation of the leakage current. Several donors and acceptors which are charged at room temperature could be identified. These defects are mainly produced in heavily damaged regions with high defect concentrations (*cluster*). The origin of trapping has not been found until today, but recent results show a possible correlation to the same cluster related defects.
This article describes the approaches and measurement methods which are used in the present defect investigations. In addition, an overview is given about the results of defect investigations.

The 20th Anniversary International Workshop on Vertex Detectors - VERTEX 2011
June 19 - 24, 2011
Rust, Lake Neusiedl, Austria

[*]Speaker.
[†]The author wishes to thank D. Eckstein, E. Fretwurst, M. Moll and I. Pintilie.

© Copyright owned by the author(s) under the terms of the Creative Commons Attribution-NonCommercial-ShareAlike Licence. http://pos.sissa.it/

PoS(Vertex 2011)035

1. Introduction

Silicon sensors are widely used in tracking detectors of high energy physics experiments. The unique knowledge about this material and the proven technology makes it first choice for large scale applications. The upgrade of the large hadron collider (LHC) to the *high luminosity* (HL) LHC will increase the integrated luminosity by a factor of five and therefore the radiation exposure to a maximum fluence of more than $\Phi = 10^{16}$ cm^{-2}.
The radiation induced bulk damage in the silicon sensors will lead to a severe degradation of their performance during the operational time. The introduction of defect levels in the band gap (E_g) change the properties of silicon sensors, leading to an increase of the leakage current (I_{leak}), a decrease of the charge collection efficiency (*CCE*) and a change of the depletion voltage (V_{dep}). These changes finally result in a loss of efficiency and resolution.
One approach for improving the radiation tolerance of silicon sensors is based on the understanding of radiation damage in the silicon bulk. The goal of such analysis is firstly to be able to predict the properties of the irradiated sensors correctly and secondly to be able to carry out defect engineering. Defect engineering aims to render inactive harmful defects by the intentional introduction of impurities. Today's standard material used in the LHC tracking detectors is oxygen enriched silicon. The beneficial influence of oxygen on the change of the effective doping concentration (N_{eff}) and therefore also on V_{dep} was explained by the CERN-RD48 (ROSE) collaboration [1] on the basis of defect investigations.
From the work of the ROSE collaboration emerged a full characterisation of the radiation induced defects in ^{60}Co-γ irradiated sensors [2–6]. For the first time, the generation of I_{leak} and the change of N_{eff} could be predicted by defect analysis.
Since the radiation induced damage of ^{60}Co-γ irradiation only generates small point defects, a similar approach had to be started for HL LHC conditions where mainly large damage cascades are created [7–9]. The main deterioration of the silicon sensors results from the influence of these large defect conglomerations, the *clusters*, as introduced by 1 MeV neutron or 23 GeV proton irradiation [6,10,11]. Fig. 1 presents the simulation of a *primary knock on atom* (PKA) path (red) through silicon creating an avalanche cascade of vacancy displacements (blue). As indicated in the figure, the cluster regions are found at the end of the damage cascade, where the energy of the displaced silicon atoms decrease.
The investigation of radiation induced defects can be achieved by a comparison of the change of the relevant diode properties (depletion voltage (V_{dep}), leakage current (I_{leak}), trapping ($\tau_{n,p}$)) with defect properties (defect concentration (N_t), capture cross section ($\sigma_{n,p}$), activation energy (ΔE_a)). These values can be obtained on one hand by capacitance-voltage (CV) and current-voltage characteristics (IV) and on the other hand *Deep Level Transient Spectroscopy* (DLTS) and *Thermally Stimulated Current technique* (TSC). A correlation of such values can be achieved during annealing procedures. The electrical analysis methods for investigating the defect properties require planar diode test-samples irradiated with neutrons and protons to comparatively low fluences from $\Phi = 10^{11} - 10^{15}$ cm^{-2}. Materials with different concentrations of impurities may give further information about their influence on the defect generation and the impact on detector properties.

PoS(Vertex 2011)035

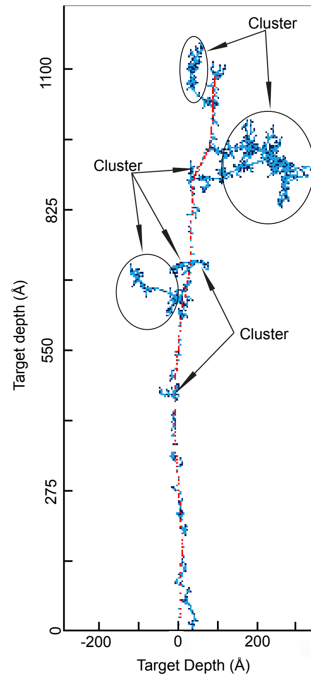

Figure 1: Simulation of the path of a primary dislocated silicon atom, a PKA (red) through silicon creating an avalanche cascade of vacancy displacements (blue). Figure from [11].

2. Experimental Methods and Materials

Defect investigations aim to understand radiation induced bulk damage depending on the irradiating particle, the fluence and the silicon material. Understanding the generation of defects makes it possible to forecast the change of sensor properties (V_{dep}, I_{leak}, $\tau_{n,p}$) and to choose the best material for a sensor's position in the detector. Additionally, the information about the chemical structure of a defect allows to perform defect engineering.
Defect engineering seeks to improve the radiation hardness of silicon sensors by the intentional incorporation of impurities in order to de-activate harmful defects. A "result" of defect engineering is oxygen enriched silicon. The understanding of the beneficial impact of oxygen in n-type silicon was the basis for the big success of this material, which is now widely used in LHC experiments.
Several defect reactions with positive impact on the radiation hardness can be observed (for $[O] > 10^{17}$ cm^{-3}). One example is pictured in Fig. 2. The radiation induced vacancy defect (V) usually couples with either other vacancies or the material impurities present in the silicon material. Depending on the concentration of such, some reactions are more prominent than others. In the case of oxygen lean material a phosphorus substitutional atom (P_s) can form the vacancy-phosphorus-complex (VP) with the irradiation induced vacancy. This defect is harmful because the phosphorus atom (usually acting as donor) becomes inactivated and does not contribute to N_{eff}. However in oxygen rich silicon, like epitaxially grown (Epi-Do) or Magnetic Czochralski (MCz) silicon, due to the excessive supply of oxygen atoms (O_i) the formation of the vacancy-oxygen-complex (VO_i) is favoured. Neither the oxygen atom nor the phosphorus dopant is mobile at room temperature or at 80 °C annealing, but the vacancy migrates through the lattice even at lower temperatures and

PoS(Vertex 2011)035

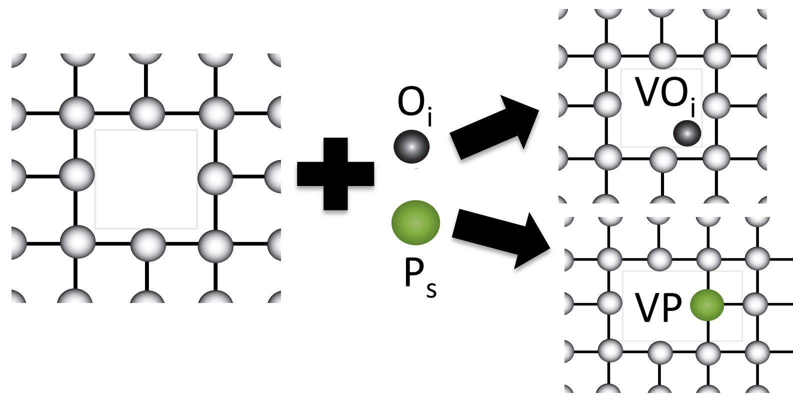

Figure 2: Illustration of reactions of radiation induced vacancys (V) with either an oxygen atom (O_i) or phosphorus atom (P_s). O_i + V creates harmless vacancy-oxygen-complex (VO_i) while $V + P_s$ creates the inactive vacancy-phosphorus defect (VP), which decreases the initial doping concentration.

therefore couples with the impurities. If $[O] \gg [P]$ it is much more likely that a vacancy couples with oxygen than with the phosphorus doping atom.

Knowledge about the defects in the silicon bulk can be obtained with material studies and measurement methods from solid state physics. A very powerful tool for obtaining defect properties, like N_t, ΔE_a and $\sigma_{n,p}$, is the deep level transient spectroscopy DLTS. This method was proposed by Lang [12] and is described in Weiss [13] and Moll [10]. The method is based on capacitance differences due to the emission of charge carriers from filled trap levels. This requires a high majority carrier concentration and is therefore only applicable for sensors with $N_{eff,0} \gg N_t$, limiting the irradiation fluences to $\Phi_{eq} = 6 \times 10^{11}$ cm^{-2} for the sensors under investigation. Here $N_{eff,0}$ denotes the original doping concentration. A second method, the thermally stimulated current technique (TSC), is based on a direct measurement of the current emission from filled traps (for more information see [14–16]). Therefore, sensors with higher irradiation fluences of $\Phi_{eq} = 10^{13} - 10^{15}$ cm^{-2} are feasible.

Annealing studies mimic the self-healing process of the silicon bulk during maintenance times with acceleration factors depending on the applied temperature and compared to room temperature annealing. It should be noted, that acceleration factors for the annealing of I_{leak} differ from the annealing of N_{eff}. A parameterisation of the annealing of N_{eff} including acceleration factors for the short term and the long term annealing is given in Moll [10]. Additional annealing processes at high temperature allow the observation of migration and dissolving processes in the silicon bulk. It is possible to distinguish the chemical structure from such experiments.

The planar diodes used for studying radiation damage are made of the silicon materials which differ in oxygen concentration $[O]$, general impurity content (like carbon) and original doping concentration $N_{eff,0}$. Materials with a low oxygen content resulting from the growth process are float zone (FZ) and standard epitaxially (Epi) grown silicon, with concentrations of $[O] \approx 10^{16}$ cm^{-3}. Oxygen rich silicon materials like Magnetic Czochralski (MCz) or oxygen enriched epitaxial silicon (Epi-Do) and oxygen enriched float zone (DOFZ) have concentration between $[O] \approx 2 \times 10^{17} - 5 \times 10^{17}$ cm^{-3}. 23 GeV irradiations have been carried out at the Proton Synchrotron (PS) [17, 18] at CERN and 1 MeV neutron irradiations at the JSI Ljubljana [19].

PoS(Vertex 2011)035

3. Results

In recent years, progress was made especially in the identification of defects with impact on the leakage current and the change of the effective doping concentration after the irradiation with neutrons and charged hadrons. Several defect candidates could be correlated to the respective diode properties due to a comparison of their properties during annealing studies. The knowledge about defects with impact on the sensor properties is summarised in this section.

3.1 Effective doping concentration

The depletion voltage V_{dep} and similarly N_{eff} (connected via $V_{dep} = \frac{q_0}{\varepsilon\varepsilon_0} \cdot |N_{eff}| \cdot d^2$) are known to change as a result of radiation damage, depending on material and the doping-type. As a consequence for a sensor in a high energy physics detector, it is possible that V_{dep} rises so that the biasÊ voltage that can be applied is not sufficient to deplete the sensors fully. Additionally, the materials can undergo type inversion. If a type inverted sensor cannot be depleted any more. Therefore it is vital to estimate the evolution of V_{dep} depending on the fluence and the particle type. A basic approach is the understanding of radiation induced defects responsible for the change of N_{eff}.
In the recent years, several defects with impact on V_{dep} have been identified due to their Poole-Frenkel-Effect. Only defects that are charged at room temperature contribute to N_{eff} exhibiting a field dependence (see [6,20]). Nearly all these investigations were performed on n-type silicon, but since radiation induced defects are similar for n- and p-type material, radiation induced defects are supposed to be similar for both types. However, the difference between the phosphorus and boron doping atoms leads to the creation of different defect complexes, resulting in a different behaviour mostly at low fluences ($\Phi_{eq} < 10^{14}$ cm^{-3}), where the original doping concentration is relevant.
Major progress was made by Pintilie et al. [6, 21] finding the main reason for type inversion of n-type sensors after 1 MeV neutron irradiation. Pintilie et al. found a group of radiation induced deep acceptors displayed in the TSC curve of a neutron irradiated (blue) oxygen enriched epitaxially grown planar silicon diode illustrated in Fig. 3. The deep acceptors are labelled with respect to their level's peak position in the TSC spectra $H(116K)$, $H(140K)$ and $H(151K)$ (at $E_a = 0.33$ eV, $E_a = 0.36$ eV and $E_a = 0.42$ eV [6]). These deep acceptors were also found in 23 GeV proton irradiated silicon (see Fig. 3 red curve).
In addition, a shallow donor with impact on the N_{eff} has been identified. This defect was labelled $E(30K)$ (at $E_a = 0.1$ eV) according to its TSC peak position [6]. It can be found for both neutron and proton irradiation. The comparison of TSC spectra illustrated in Fig. 3 taken at the same annealing step of 30 000 minutes at 80 °C and normalised to an equivalent fluence of $\Phi_{eq} = 2 \times 10^{14}$ cm^{-2} reveals the main difference between bulk defects induced by 1 MeV neutron and 23 GeV proton irradiation. The concentration of the $E(30K)$ defect is much higher after 23 GeV proton irradiation.
For a full description of the change of N_{eff} based on defects, two further defects have to be taken into account. A shallow donor, labelled as BD defect and the above mentioned VP defect change the effective doping concentration. BD was identified to be $TDD2$ [4, 5, 20], appearing only in oxygen rich or medium oxygen rich silicon. VP on the other hand is mostly suppressed in oxygen

PoS(Vertex 2011)035

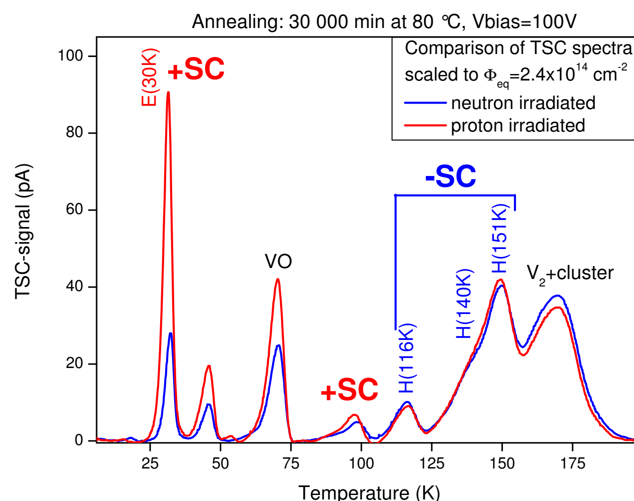

Figure 3: Comparison of defect peaks measured by TSC for 1 MeV neutron (blue) and 23 GeV proton (red) irradiated oxygen enriched epitaxially grown silicon material. Defects with impact on N_{eff} are marked with +SC for donors and -SC for acceptors. (Measurement conditions: $V_{meas} = 100$ V, $V_{pulse} = -50$ V.) Figure from [11].

rich material.
The identification of the defects can be nicely confirmed by annealing studies. If the identified defects should be responsible for a change of N_{eff}, it would be possible to reproduce N_{eff} measured by CV at room temperature by the sum of all defect concentrations observed by microscopic measurement techniques during annealing studies.
Figure 4 illustrates the TSC spectra taken during an isothermal annealing study of a standard epitaxially grown silicon diode for bias voltages of $V_{bias} = 100$ V. The acceptors with impact on N_{eff} are marked in blue ($H(116K)$, $H(140K)$ and $H(151K)$), donors in red ($E(30K)$ and BD). The area under a TSC-peak in the spectrum gives the concentration of the defect. Both, the concentration of acceptors and donors increase with annealing at 80 °C.
The results of the evaluation during the annealing process are presented in Fig. 5. The concentrations of donors were summed up and displayed as positive concentration by red triangles, while the sum of the concentration of acceptors is illustrated by blue circles. Since acceptors contribute negatively to the space charge, they are represented on a negative scale.
The effective doping concentration can then be calculated from the sum of the original doping $N_{eff,0}$, the concentration of all acceptors, donors and VP (E-center). This is illustrated by green stars. The annealing behaviour of N_{eff} measured by CV at room temperature can be reproduced very accurately by the concentrations of the identified defects. However, it should be noted that for higher fluences and oxygen enriched material, only the long term annealing is reproduced by the defect analyses.

3.2 Current

The increase of the leakage current after irradiation will become a severe problem for sensors

PoS(Vertex 2011)035

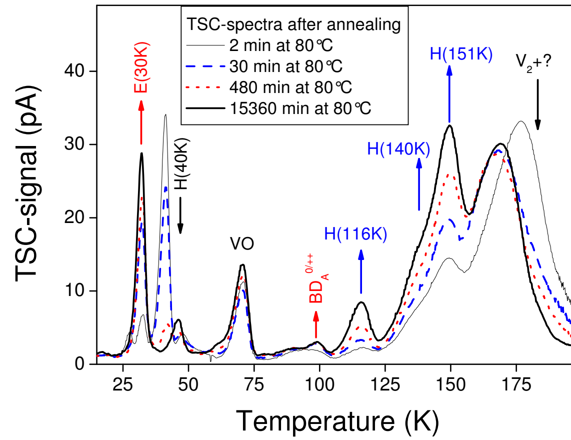

Figure 4: TSC spectra of $\Phi = 2 \times 10^{14}$ cm^{-2} neutron irradiated standard epitaxially grown material, measurement during heating at $V_{bias} = 100$ V. Figure from [11].

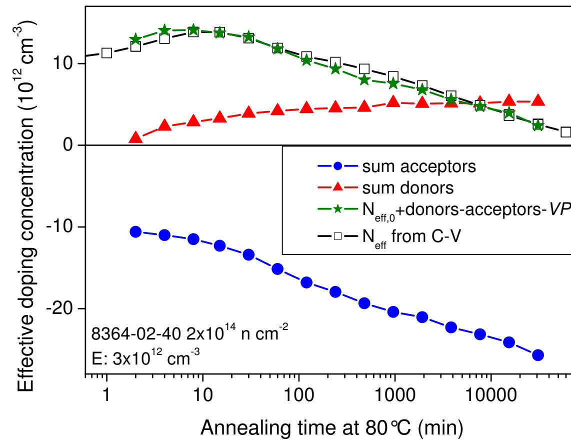

Figure 5: Concentrations of defects influencing N_{eff}, evaluated from TSC spectra of $\Phi_{eq} = 2 \times 10^{14}$ cm^{-2} neutron irradiated standard epitaxially grown material. The sum of the concentrations (green stars) deduced from concentrations of acceptors (blue circles), donors (open black squares) and the VP (E-center) and $N_{eff,0}$ is compared to N_{eff} from CV at room temperature for isothermal annealing studies at 80 °C. Figure from [11].

in tracking detectors at the future HL LHC. The increase of I_{leak} results in an increase of shot noise and to a reduction of the signal to noise ratio. To today, I_{leak} showed no dependence on the material (see Moll [10]).

This section addresses the identification of defects that are responsible for the increase of I_{leak} after neutron and charged hadron irradiation. Besides defect properties and the annealing behaviour also the knowledge of the chemical structure of defects with impact on I_{leak} is a matter of interest. This information increases the prospects for developing future materials that are less susceptible for radiation damage, after all.

Currently the noise is reduced and controlled by cooling the detectors. This approach works very well but has some disadvantages. An active cooling system makes a large contribution to the material budget and hence to the multiple scattering, it is limited to the minimum cooling temperature

PoS(Vertex 2011)035

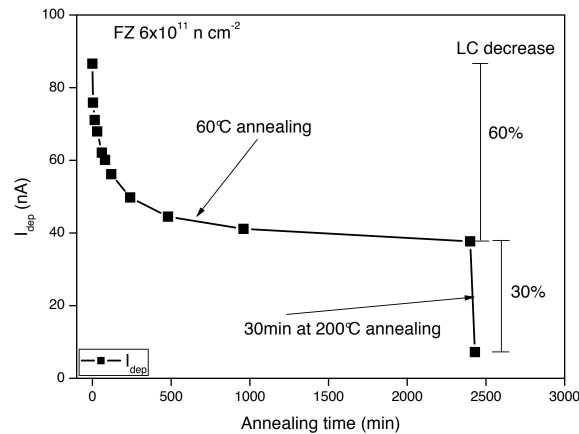

Figure 6: Current decrease during the annealing at 60°C and 200°C. A major portion of 60 % of the initial I_{leak} decreases during 60°C annealing for 2400 min and additional 30 % during 30 minutes at 200 °C. Figure from [11].

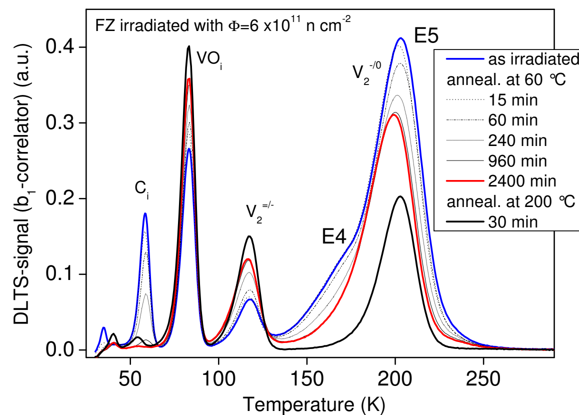

Figure 7: Annealing behaviour of defects at 60 °C in a 100 µm thick FZ planar diode irradiated with $\Phi = 6 \times 10^{11}$ n cm^{-2} measured by DLTS. Measurement conditions: $V_R = -10$ V, $V_P = -0.1$ V, $t_w = 200$ ms. Figure from [11].

and prone to failure of the cooling system.

IV measurements during annealing studies point out impressively that the main part of I_{leak} anneals out within a few hundred minutes annealing at 60 °C. Fig. 6 illustrates an annealing study performed on $\Phi = 6 \times 10^{11}$ neutron cm^{-2} irradiated FZ diodes with two temperature steps. At first, several isothermal annealing steps were done at 60 °C up to 2400 minutes, followed by an annealing step of 30 minutes at 200 °C. The annealing treatment at 60 °C results in a first decrease of I_{leak} of about 60 %. A second drop can be observed after the annealing at a higher temperature. After annealing for 30 minutes at 200 °C I_{leak} decreases for another 30 %.

Since the annealing of I_{leak} is a result of the dissolving of defects in the silicon crystal, it should be possible to see the decrease of the concentration of these defects during an annealing study. Corresponding DLTS spectra, taken during the annealing treatment and always after CV/IV measurements, are presented in Fig. 7. In a DLTS spectrum each peak position and height represents the concentration of the defect at a level in the band gap. For this sample the defect levels for

PoS(Vertex 2011)035

several defects without influence on the electrical properties of the silicon were observed (C_i, VO_i and V_2).
Defects with impact on I_{leak} have to have deep levels, near to the middle of the band gap. In this presentation, the large defect peak around 200 K is deep enough to contain a generation centre. During the annealing process it becomes obvious that the large peak consists of several defects that dissolve as a function of the annealing time and temperature. The peak height gives the concentration of a defect. Therefore it is possible to calculate the annealed fraction from the difference of the peak height at respective annealing temperatures or time steps.
Figure 7 illustrates the annealing of two defect levels at 60 °C in addition to a further defect level which anneals during the 30 minutes at 200 °C step. The original concentration of defects can be pictured by taking the difference of the spectra directly after irradiation and the succeeding annealing steps as depicted in Fig. 8. The difference between the *as irradiated* step and the longest annealing step reveals the concentration of the $E5$ defect.
At each annealing step, the annealed fraction of the defect concentration can hence be extracted and correlated to the annealed fraction of I_{leak}. Fig. 9 demonstrates the annealing of the $E5$ defect concentration ($\Delta N_t(E5)$) and the annealing of the current damage parameter ($\Delta\alpha$). This parameter can be obtained by normalising the radiation induced leakage current (ΔI) by the diode volume (V) and the fluence ($\alpha = \Delta I/V \cdot \Phi_{eq}$, compare [10]). The materials combined in Fig. 9 represent the isochronal annealing steps at 60 °C for MCz, FZ, Epi-St and Epi-Do materials. A linear trend can be observed.
This defect has been known for a long time [10], though only recently could it be directly correlated to the annealing of the current by utilising the newly discovered bistability of this defect [22–24].
The authors found that the defect is not dissolved after annealing at 80 °C but changed the configuration. This configuration gives only rise to a shallow defect ($E75$) of which the contribution to the current generation is negligible. An injection of high forward current of 1 A ($J = 4$ A cm^{-1}) recovers the configuration that gives rise to the deep level $E5$ [11, 24]. As demonstrated in [11], the recovery of the defect concentrations also recovers a fraction of the leakage current. Using this bistability makes it possible to investigate the defect dissociation at higher temperatures. Recent investigations revealed the chemical structure of the defect to be the tri-vacancy (V_3) [11,25]. This is in agreement with the observation that the generation of this defect does not depend on the material and should consist only of silicon vacancies or interstitials.
There was a second defect observed during the high temperature annealing step that was labelled $E205a$. Analogously to that shown in Fig. 7 this defect can be correlated to the decrease of the leakage current during the annealing at higher temperatures [11].
The $E205a$ defect is also under suspicion to be responsible for electron trapping after hadronic irradiation. This defect is the only defect that anneals exactly in the same temperature range as the electron trapping gets reduced due to annealing [26].

4. Conclusion

Some defects with impact on N_{eff} and I_{leak} after the irradiation with 1 MeV neutrons and 23 GeV protons have been successfully revealed by defect investigations. The deep acceptors $H(116K)$, $H(140K)$ and $H(151K)$ appear to have the same generation rate after neutron and pro-

PoS(Vertex 2011)035

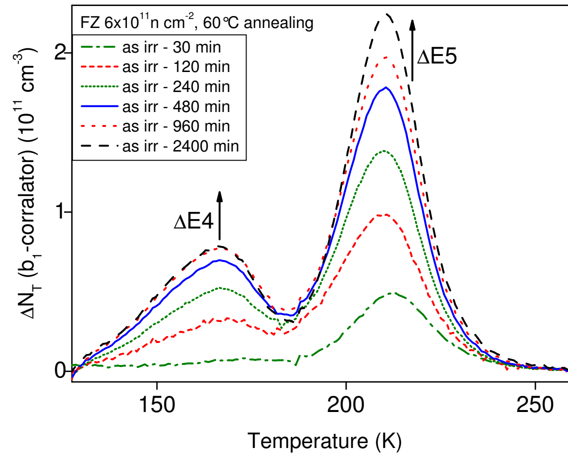

Figure 8: Annealing behaviour of the $E4/E5$ defect levels at 60 °C in a 100 µm thick FZ sensor, irradiated with $\Phi = 6\times10^{11}$ n cm^{-2} measured by DLTS. The presented spectra illustrate the fraction of the annealed defects from the difference of the *as irradiated* measurement and a succeeding annealing step. Measurement condition: $V_R = -10$ V, $V_P = -0.1$ V, $t_w = 200$ ms. Figure from [11].

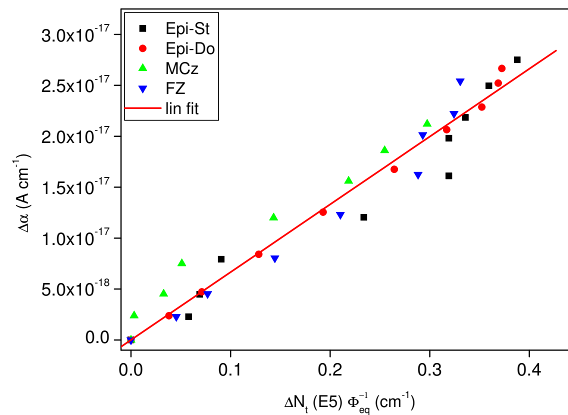

Figure 9: Correlation of the $E5$ defect concentration with the change in the damage parameter α for Epi-St, Epi-Do, Mcz and FZ material all irradiated with 1 MeV neutrons, normalised. Figure from [11].

ton irradiation and in addition to the VP defect lead to type inversion of neutron irradiated sensors. The production of the donors $E(30K)$ and BD is enhanced after 23 GeV proton irradiation. The production of the BD defect is furthermore enhanced in oxygen rich material. This high generation explains the observation, that oxygen enriched epitaxial silicon diodes do not undergo type inversion after proton irradiation. It is possible to explain also the similar behaviour of n-type MCz material after proton irradiation, since the material properties are very similar.
The high leakage current after hadronic irradiation was correlated to two cluster related defects. The current is created by the tri-vacancy and the $E205a$ defect and their interaction with the whole cluster region (e.g. by inter center charge transfer [27]). Since the tri-vacancy is very stable until high temperatures ($T > 250$ °C) it does not couple with oxygen. Therefore no beneficial effect of oxygen on the leakage current is expected. There are two other candidate impurities for defect engineering, which are nitrogen and hydrogen. However, neither a sufficient enrichment of silicon

PoS(Vertex 2011)035

with either of the impurities nor the influence of the radiation hardness has been tested yet. Therefore the cooling of silicon sensors remains the only possible control of I_{leak}. A detailed study of these defects and their interaction with other impurities than oxygen will offer the possibility of an estimation of a possible success of future defect engineering for radiation hardness. A compilation of ΔE_a, $\sigma_{n,p}$ for defects with impact on N_{eff} and I_{dep} can be found in [11].
The understanding of the correlation of the defect introduction depending on the irradiation can be used to predict the properties of irradiated sensors. A prediction helps to choose the best material for a certain fluence range and a particle composition. The prediction of type inversion or non type inversion gives an impact on the design of a sensor as well as the prediction of V_{dep} that is necessary to keep the operation voltages in design specifications. An application of this knowledge on p-type sensors is strictly speaking only possible for high fluences ($\Phi > 10^{14}$) when the original doping concentration does not count any more.

PoS(Vertex 2011)035

5. Summary

Defect analysis have been of great benefit in order to understand the effects of radiation damage in the silicon bulk. Several defects were found that influence the effective doping concentration. Furthermore, two defects affecting the leakage current were identified. It is likely that they interact with the cluster region, e.g. by inter center charge transfer. The understanding of the impact of these defects will make it possible either to carry out defect engineering or to estimate the change of N_{eff} and I_{leak} depending on the type and amount of radiation they were exposed to. The prediction of a possible type inversion can be made for materials whose oxygen content and original doping concentration are known. A compilation of ΔE_a, $\sigma_{n,p}$ for defects with impact on N_{eff} and I_{dep} can be found in [11].

6. Acknowledgements

A large fraction of this work was performed in the frame of the CERN-RD50 collaboration and funded by the CiS-Hamburg project under Contract No. SSD 0517/03/05. It was supported by the German BMBF foundation in the frame of the FSP102 (CMS) and the Helmholtz Alliance: Physics at the Terascale. The author would like to thank especially V. Cindro and G. Kramberger for the neutron irradiation and M. Glaser who provided the 24 GeV/c proton irradiations. The author owes further thanks to D. Eckstein, E. Fretwurst, M. Moll and I. Pintilie.

References

[1] The ROSE Collaboration, R & D On Silicon for future Experiments, CERN-RD48 Collaboration.

[2] I. Pintilie, E. Fretwurst, G. Lindström, J. Stahl, Close to midgap trapping level in ^{60}Co gamma irradiated silicon detectors, Appl. Phys. Lett. 81 (1) (2002) 165–167.

[3] I. Pintilie, E. Fretwurst, G. Lindström, J. Stahl, Second-order generation of point defects in gamma-irradiated float-zone silicon, an explanation for “type inversion”, Appl. Phys. Lett. 82 (13) (2003) 2169–2171.

[4] I. Pintilie, E. Fretwurst, G. Lindström, J. Stahl, Results on defects induced by ^{60}Co gamma irradiation in standard and oxygen-enriched silicon, NIM A 514 (2003) 18–24.

[5] I. Pintilie, E. Fretwurst, G. Kramberger, G. Lindström, Z. Li, J. Stahl, Second-order generation of point defects in highly irradiated float zone silicon–annealing studies, Physica B 340–342 (2003) 578–582.

[6] I. Pintilie, G. Lindstroem, A. Junkes, E. Fretwurst, Radiation-induced point- and cluster-related defects with strong impact on damage properties of silicon detectors, NIM A 611 (2009) 52–68.

[7] M. Huhtinen, P. Aarino, Estimation of pion induced displacement damage in silicon, HU-SEFT R 1993-02.

[8] M. Huhtinen, P. Aarino, Pion induced displacement damage in silicon devices, NIM A 335 (1993) 580.

[9] M. Huhtinen, Simulation of non-ionising energy loss and defect formation in silicon, NIM A 491 (2002) 194–215.

[10] M. Moll, Radiation Damage in Silicon Particle Detectors - microscopic defects and macroscopic properties -, Ph.D. thesis, Universität Hamburg, DESY-THESIS-1999-040 (December 1999).

[11] A. Junkes, Influence of radiation induced defect clusters on silicon particle detectors, Ph.D. thesis, Universität Hamburg, DESY-THESIS-2011-031 (July 2011).

[12] D. V. Lang, Deep-level transient spectroscopy: A new method to characterize traps in semiconductors, J. Appl. Phys. 45 (7) (1974) 3023–3032.

[13] S. Weiss, Halbleiteruntersuchungen mit dem DLTFS- (Deep Level Transient Fourier Spectroscopy) Verfahren, Ph.D. thesis, Universität Kassel (January 1991).

[14] I. R. Weisenberg, H. Schade, A technique for trap determinations in low-resistivity semiconductors, J. Appl. Phys. 39 (11) (1968) 5149–5151.

[15] L. Forbes, C. T. Sah, On the determination of deep level center energy and concentration by thermally stimulated conductivity measured using reverse-biased p-n junctions, Solid-State Electron. 14 (1971) 182–183.

[16] I. Pintilie, L. Pintilie, M. Moll, E. Fretwurst, G. Lindström, Thermally stimulated current method applied on diodes with high concentration of deep trapping levels, Appl. Phys. Lett. 78 4 (2001) 550–552.

[17] M. Glaser, L. Durieu, F. Lemeilleur, M. Tavlet, C. Leroy, P. Roy, New irradiation zones at the CERN-PS, NIM A 426 (1999) 72–77.

[18] M. Glaser, F. Ravotti, M. Moll, Dosimetry Assessments in the Irradiation Facilities at the CERN-PS Accelerator, IEEE Transaction on Nuclear Science 53 No. 4 (2006) 2016–2022.

[19] Jožef Stefans Institute Ljubljana and Department of Physics, University of Ljubljana, SI-1000 Ljubljana, Slovenia.

[20] I. Pintilie, M. Buda, E. Fretwurst, G. Lindström, J. Stahl, Stable radiation-induced donor generation and its influence on the radiation tolerance of silicon diodes, NIM A 556 (2006) 197–208.

[21] I. Pintilie, E. Fretwurst, G. Lindström, Cluster related hole traps with enhanced-field-emission-the source for long term annealing in hadron irradiated Si diodes, Appl. Phys. Lett. 92 (2008) 024101.

[22] R. M. Fleming, C. H. Seager, D. V. Lang, E. Bielejec, J. M. Campbell, Defect-driven gain bistability in neutron damaged, silicon bipolar transistors, Appl. Phys. Lett. 90 (2007) 172105.

PoS(Vertex 2011)035

[23] R. M. Fleming, C. H. Seager, D. V. Lang, P. J. Cooper, E. Bielejec, J. M. Campbell, Effects of clustering on the properties of defects in neutron irradiated silicon, J. Appl. Phys. 102 (2007) 043711.

[24] A. Junkes, D. Eckstein, I. Pintilie, L. F. Makarenko, E. Fretwurst, Annealing study of a bistable cluster defect, NIM A 612 (2010) 525–529.

[25] V. P. Markevich, A. R. Peaker, S. B. Lastovskii, L. I. Murin, J. Coutinho, V. J. B. Torres, P. R. Briddon, L. Dobaczewski, E. V. Monakhov, B. G. Svensson, Trivacancy and trivacancy-oxygen complexes in silicon: Experiments and ab initio modeling, Phys. Rev. B 80 (2009) 235207.

[26] M. K. Bock, Isochronal annealing studies on neutron irradiated silicon detectors, Diploma Thesis, Universität Hamburg (November 2008).

[27] K. Gill, G. Hall, B. MacEvoy, Bulk damage effects in irradiated silicon detectors due to clustered divacancies, J. Appl. Phys. 82 (1) (1997) 126–136.

PoS(Vertex 2011)035